Analysis of Two Dimensional Steady-State Heat Conduction Problems by MLPG Method

Gholam Hosein Bradaran
Department of Mechanical Engineering,
Shahid Bahonar University, Kerman, Iran
E-mail: Barao2002@ yahoo.com

Mohammad Javad Mahmoodabadi*
Department of Mechanical Engineering,
Guilan University, Rasht, Iran
E-mail: mahmood_1985_mj@yahoo.com
*Corresponding author

Received 26 May 2011; Revised 28 August 2011; Accepted 19 September 2011

Abstract: Numerical solutions obtained by the Meshless local Petrov–Galerkin (MLPG) method are presented for two-dimensional steady-state heat conduction problems. The MLPG method is a truly meshless approach, and neither the nodal connectivity nor the background mesh is required for solving the initial-boundary-value problem. The penalty method is adopted to efficiently enforce the essential boundary conditions, the moving least squares approximation is used for interpolation schemes and the Heaviside step function is chosen for test function. The results show that the present method is very promising in solving engineering two-dimensional steady-state heat conduction problems.

Keywords: Heat Conduction, Heaviside Step Function, Meshless Local Petrov–Galerkin, MLS.

Reference: Gh. H. Baradaran and M. J. Mahmoodabadi, (2011) 'Analyze of Tow-Dimensional Steady-State Heat Conduction Problems by MLPG Method', Int J Advanced Design and Manufacturing Technology, Vol. 4/ No. 4, pp. 47-56.

Biographical notes: Gh. H. Baradaran received his PhD in Mechanical Engineering from University of Shiraz. He is currently Assistant Professor at Mechanical Engineering Department, Shahid Bahonar University, Kerman, Iran. His current research interest includes Elasticity, Plasticity, FEM and Meshfree Methods. **M. J. Mahmoodabadi** is PhD student of Mechanical Engineering at the University of Guilan, Iran. He received his MSc and BSc in Mechanical Engineering from Shahid Bahonar University of Kerman, Iran. His current research focuses on Numerical Method, Linear and Nonlinear Control, Optimization and Fuzzy Systems.

1 INTRODUCTION

In recent years, the meshless method has emerged as an effective numerical approach to find solutions of initial-boundary-value problems. The Meshless Local Petrov–Galerkin (MLPG) method is one of the meshless schemes. The main advantage of this method compared with other meshless methods is that no background mesh is used to evaluate various integrals appearing in the local weak formulation of problem. Therefore, this method is a "truly meshless" approach in terms of both interpolation of variables and integration of energy. The MLPG method has been demonstrated to be quite successful in solving different branches of initial-boundary-value problems. Atluri and Zhu [1] solved elastostatic problems, Lin and Atluri [2] introduced the up winding scheme to analyze steady state convection–diffusion problems, and Liu and Gu [3] coupled the MLPG method with either the finite element or the boundary element method to enhance the efficiency of the MLPG method. Ching and Batra [4] augmented the polynomial basis functions with singular fields to determine deformations and stress fields near the crack tip for generally 2-D mixed-mode problems. Liu and Gu [3] and Ching and Batra [4] used the Newmark family of methods to analyze 2-D transient elastodynamic problems. The bending of a thin plate has been studied by Liu and Gu [3] and Long and Atluri [5], and Cleary et al. [6] scrutinized deformations of a material compressed in a rough rectangular cavity. Qian et al. [7] combined the MLPG method with a higher-order shear and normal deformable plate theory to analyze static deformations, free and forced vibrations of rectangular homogeneous and Functionally Graded (FG) plates. The objective of this work is to present the MLPG analysis for two-dimensional steady-state heat conduction problems. First, we list governing equations next, the weak formulations of MLPG method and the moving least squares (MLS) approximation is briefly introduced.

2 MLPG FORMULATION

We consider a 2D Heat Conduction problem, as shown in Fig. 1, for illustrating the procedure for formulating the MLPG method. The problem domain is denoted by Ω, which is bounded by boundaries including essential boundary Γ_1, natural boundary Γ_2 and Robin boundary Γ_3 In the MLPG method, the problem domain is represented by a set of arbitrarily distributed nodes, as shown in same. The weighted residual method is used to create the discrete system equation.

The major idea in MLPG is that the implementation of the integral form of the weighted residual method is confined to a very small local sub-domain of a node. This means that the weak form is satisfied at each node in the problem domain in a local integral sense. Therefore, the weak form is integrated over a "local quadrature domain" that is independent of other domains of other nodes. This is made possible by use of the Petrov-Galerkin formulation, in which one has the freedom to choose the test and trial functions independently**.**

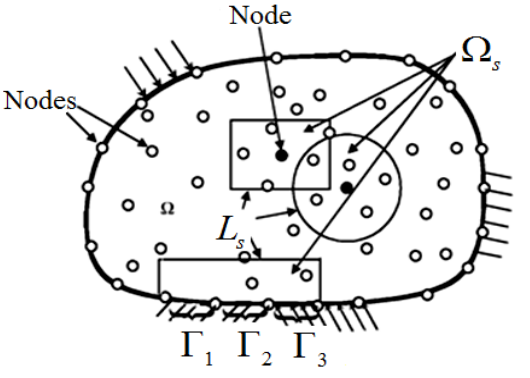

Fig. 1 Domains and their boundaries

The heat conduction Poisson equation and boundary conditions can be written as

$$\lambda \frac{\partial^2 \theta}{\partial x^2} + \lambda \frac{\partial^2 \theta}{\partial y^2} = \dot{\psi} \quad in\ \Omega \tag{1}$$

The Dirichlet boundary condition:

$$\theta = \theta_1 \quad on \quad \Gamma_1 \tag{2}$$

The Neumann boundary condition:

$$-\lambda\left(\frac{\partial \theta}{\partial x} n_x + \frac{\partial \theta}{\partial y} n_y\right) = q \quad on \quad \Gamma_2 \tag{3}$$

The Robin boundary condition:

$$-\lambda\left(\frac{\partial \theta}{\partial x} n_x + \frac{\partial \theta}{\partial y} n_y\right) = h(\theta_f - \theta) \quad on \quad \Gamma_3 \tag{4}$$

where θ represents temperature, λ the thermal conductivity, n_x and n_y are the component the outward unit vector to Γ, q the given heat flux, h the convection heat transfer coefficient θ_f is the

environmental temperature, $\dot{\psi}$ the heat source per unit mass, and Γ_1, Γ_2 and Γ_3 the boundaries at which the Dirichlet, Neumann and Robin conditions apply, respectively.

In the Ω_s, the weighted integral form of Eq. (1) is given as

$$\int_{\Omega_s} \lambda[(\frac{\partial^2\theta}{\partial x^2}+\frac{\partial^2\theta}{\partial y^2})-\dot{\psi}]\nu d\Omega_s = 0 \quad (5)$$

Where ν is test function. To reduce this high-order differentiability requirement on θ, we can integrate Eq. (5) by parts. By using Gauss's theorem, we can obtain the following local weak formulation equation:

$$\int_{\Omega_s}(\lambda\frac{\partial\theta}{\partial x}\frac{\partial\nu}{\partial x}+\lambda\frac{\partial\theta}{\partial y}\frac{\partial\nu}{\partial y}+\dot{\psi}\nu)d\Omega_s$$
$$-\int_{\Gamma_1}\lambda(\frac{\partial\theta}{\partial x}n_x+\frac{\partial\theta}{\partial y}n_y)\nu d\Gamma_1$$
$$-\int_{\Gamma_s}\lambda(\frac{\partial\theta}{\partial x}n_x+\frac{\partial\theta}{\partial y}n_y)\nu d\Gamma_s = 0 \quad (6)$$

Substituting Eqs. (3) and (4) into Eq. (6), we can obtain Eq. (7).

$$\int_{\Omega_s}(\lambda\frac{\partial\theta}{\partial x}\frac{\partial\nu}{\partial x}+\lambda\frac{\partial\theta}{\partial y}\frac{\partial\nu}{\partial y}+\dot{\psi}\nu)d\Omega_s+\int_{\Gamma_2}q\nu d\Gamma_2$$
$$-\int_{\Gamma_3}h(\theta_f-\theta)\nu d\Gamma_3-\int_{\Gamma_1}\lambda(\frac{\partial\theta}{\partial x}n_x+\frac{\partial\theta}{\partial y}n_y)\nu d\Gamma_1$$
$$-\int_{\Gamma_s}\lambda(\frac{\partial\theta}{\partial x}n_x+\frac{\partial\theta}{\partial y}n_y)\nu d\Gamma_s = 0 \quad (7)$$

The MLS approximation function is given by

$$\theta=\sum_{I=1}^{N}\phi_I.\hat{\theta}_I \quad (8)$$

Substitution of Eq. (7) into Eq. (8) for all the nodes, we can obtain the following linear equations:

$$\sum_{J=1}^{M}\int_{\Omega_x}(\lambda\frac{\partial\phi^J}{\partial x}\frac{\partial\nu_I}{\partial x}+\lambda\frac{\partial\phi^J}{\partial y}\frac{\partial\nu_I}{\partial y})d\Omega_x$$
$$+\sum_{J=1}^{M}\int_{\Gamma_3}h\phi^J\hat{\theta}^J\nu_I d\Gamma_3-\sum_{J=1}^{M}\int_{\Gamma_1}\lambda(\frac{\partial\phi^J}{\partial x}n_x+\frac{\partial\phi^J}{\partial y}n_y)\nu_I d\Gamma_1$$
$$-\sum_{J=1}^{M}\int_{\Gamma_s}\lambda(\frac{\partial\phi^J\hat{\theta}^J}{\partial x}n_x+\frac{\partial\phi^J\hat{\theta}^J}{\partial y}n_y)\nu_I d\Gamma_s+\alpha\sum_{J=1}^{M}\int_{\Gamma_1}\phi^J\hat{\theta}^J\nu_I d\Gamma_1$$
$$=\int_{\Omega_x}\dot{\psi}\nu_I d\Omega_x-\int_{\Gamma_2}q\nu_I d\Gamma_2+\int_{\Gamma_3}h\theta_f\nu_I d\Gamma_3+\alpha\int_{\Gamma_1}\theta_1\nu_I d\Gamma_1 \quad (9)$$

Or

$$K.\hat{\theta}=F \quad (10)$$

Where M is the total number of nodes in the entire domain Ω, $\hat{\theta}$ the vector for the unknown fictitious nodal values, α the penalty parameter, which is used to impose the essential boundary conditions. K and F are the global stiffness matrix and the global vector, respectively, which are defined as

$$K_{IJ}=\int_{\Omega_x}(\lambda\frac{\partial\phi^J}{\partial x}\frac{\partial\nu_I}{\partial x}+\lambda\frac{\partial\phi^J}{\partial y}\frac{\partial\nu_I}{\partial y})d\Omega_x$$
$$+\int_{\Gamma_3}h\phi^J\nu_I d\Gamma_3-\int_{\Gamma_1}\lambda(\frac{\partial\phi^J\hat{\theta}^J}{\partial x}n_x+\frac{\partial\phi^J\hat{\theta}^J}{\partial y}n_y)\nu_I d\Gamma_1$$
$$-\int_{\Gamma_s}\lambda(\frac{\partial\phi^J\hat{\theta}^J}{\partial x}n_x+\frac{\partial\phi^J\hat{\theta}^J}{\partial y}n_y)\nu_I d\Gamma_s$$
$$+\alpha\int_{\Gamma_1}\phi^J\hat{\theta}^J\nu_I d\Gamma_1 \quad (11)$$

$$F_I=-\int_{\Omega_x}\dot{\psi}\nu_I d\Omega_x-\int_{\Gamma_2}q\nu_I d\Gamma_2+\int_{\Gamma_3}h\theta_f\nu_I d\Gamma_3$$
$$+\alpha\int_{\Gamma_1}\theta_1\nu_I d\Gamma_1 \quad (12)$$

3 THE MOVING LEAST-SQUARE APPROXIMATION SCHEME

Moving Least Squares (MLS), originated by mathematicians for data fitting and surface construction, can be categorized as a method of finite series representation of functions. The MLS method is now a widely used alternative for constructing meshless shape functions for approximation.

The MLS approximation has two major features that make it popular: (1) the approximated field function is continuous and smooth in the entire problem domain

and (2) it is capable of producing an approximation with the desired order of consistency. The MLS approximation is detailed in this part.

Consider a sub-domain Ω_x, which is located within the problem domain Ω (see Fig.2) and has a number of randomly located nodes x_I *(I = 1,. . . ,N)*. The moving least squares approximate $\theta^h(x)$ of $\theta(x)$ by following definition:

$$\theta^h(x) = \sum_{i=1}^{m} p(x)a(x) = p^T(x)a(x) \qquad (13)$$

Where $p^T(x)=[p_1(x),p_2(x), \ldots ,p_m(x)]$ is a complete monomial basis, m is the number of terms in the basis, and $a(x)=[a_1(x),a_2(x), \ldots ,a_m(x)]$ is the corresponding coefficient. For example, for a 2D problem, the basis can be chosen as

$$\begin{aligned} &\text{Lineae Basis}: \mathrm{p^T(x)=[1,x,y]},\ \mathrm{m=3} \\ &\text{Quadratic Basis}: \mathrm{p^T(x)=[1,x,y,x^2,xy,y^2]},\ \mathrm{m=6} \end{aligned} \qquad (14)$$

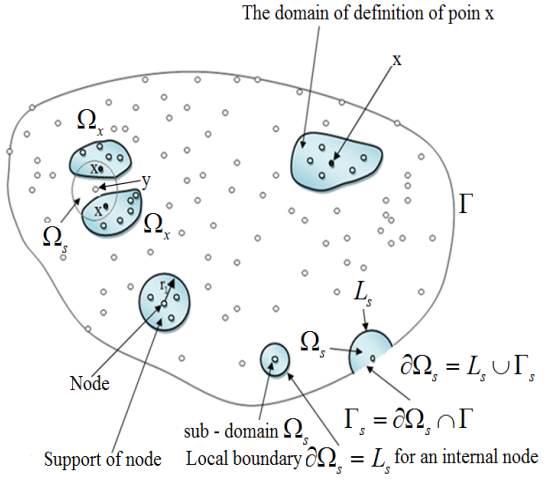

Fig. 2 Schematics of the MLS approximation

The coefficient vector a(x) is determined by minimizing the difference between the local approximation and the function, and is defined as

$$\begin{aligned} J(a(x)) &= \sum_{I=1}^{N} w_I(x)[p^T(x_I)a(x) - \hat{\theta}^I]^2 \\ &= [p\,.\,a(x) - \hat{\theta}]^T\,.W.\,[p\,.\,a(x) - \hat{\theta}] \end{aligned} \qquad (15)$$

Where x_I denotes the position vector of node *I*; $w_I(x)$ is the weight function associated with the node *I*; *N* is the number of node in Ω_x for which the weight functions $w_I(x) > 0$ are searched; the matrices **P** and **W** are defined as

$$p = \begin{bmatrix} p^T(x_1) \\ p^T(x_2) \\ . \\ . \\ . \\ p^T(x_N) \end{bmatrix} = (N \times m)\ Matrix \qquad (16)$$

$$W = \begin{bmatrix} w_1(x) & . & . & . & 0 \\ . & . & & & . \\ . & & . & & . \\ . & & & . & . \\ 0 & . & . & . & w_N(x) \end{bmatrix} = (N \times N)\ Matrix \qquad (17)$$

And

$$\hat{\theta}^T = [\hat{\theta}^1, \hat{\theta}^2, \ldots, \hat{\theta}^N] = (1 \times N)\ Vector \qquad (18)$$

In Eq. (18) $\hat{\theta}^I$ is the fictitious nodal value. It is not the nodal value of trial functions denoted by $\theta^h(x)$.

To find the coefficient a(x), we obtain the extremum by

$$\frac{\partial J(a(x))}{\partial(a(x))} = 2\sum_{I=1}^{N} w_I(x)[\sum_{I=1}^{m} p_i(x_I)a(x) - \hat{\theta}^I]p_i(x_I) = 0 \qquad (19)$$

This leads to the following set of linear relations:

$$\begin{aligned} &A(x)a(x) = B(x)\hat{\theta} \\ &(m \times m)(m \times 1) = (m \times N)(N \times 1) \end{aligned} \qquad (20)$$

Where the matrices A(x) and B(x) are defined by

$$A(x) = P^T W P = B(x)P = \sum_{I=1}^{N} w_I(x)p_I(x_I)P^T(x_I) \qquad (21)$$

$$B(x) = P^T W = [w_1(x)p(x_1), w_2(x)p(x_2), \ldots, w_N(x)p(x_N)] \qquad (22)$$

Solving a(x) from Eq. (20), and substituting it into Eq. (23), we can obtain the final form of the MLS approximation as

$$\begin{aligned} &\theta^h(x) = \Phi^T(x)\hat{\theta} = \sum_{I=1}^{N} \phi^I(x)\hat{\theta}^I \\ &\theta^h(x_I) = \theta^I \neq \hat{\theta}^I \quad , x \in \Omega_x \end{aligned} \qquad (23)$$

Where $\boldsymbol{\Phi^T(x) = p^T(x)A^{-1}(x)B(x)}$ is the shape function, and its partial derivative is :

$$\phi^{I}_{,K} = \sum_{j=1}^{m} [P_{j,k}(A^{-1}B)_{jI} + P_j(A^{-1}B_{,K} + A^{-1}_{,K}B)_{jI}] \quad (24)$$

In practical applications, the weight function $w_I(x)$ is generally nonzero over the small neighborhood of point x_I, and this neighborhood is called the domain of influence of node I (see Fig. 2). Typically, the shape of the domain in the two-dimensional space can be circular, ellipse, rectangular or any other convenient regular closed lines and in the three-dimensional space can be sphere, ellipsoid, cube or any other simple cubic volume. In the present analysis a circular domain has been selected. The choice of weight function $w_I(x)$ affects the resulting approximation $\theta^h(x)$, therefore, its selection is of essential importance. Numerical practices of [1, 2] have shown that a quadratic spline weight function works well. Hence in this article, the quadratic spline weight function is used. Thus we have

$$W_I(x) = \begin{cases} 1-6\left(\frac{d_I}{r_I}\right)+8\left(\frac{d_I}{r_I}\right)^3-3\left(\frac{d_I}{r_I}\right)^4 & 0 \le d_I \le r_I \\ 0 & d_I \ge r_I \end{cases} \quad (25)$$

Where d_I is the distance between points x and nod x_I and r_I is the size of support (see Fig.2) for the weight functions. It can be seen that the quadratic spline weight function is C^1 continuous over the entire domain.

4 ENFORCEMENT OF ESSENTIAL (DIRICHLET) BOUNDARY CONDITIONS

In MLPG shape functions do not satisfy the Kronecker delta property, and hence when such trial functions are used, it is not easy to implement the essential boundary. Various numerical techniques have been proposed to enforce the essential boundary conditions, such as the Lagrange multiplier method, the penalty approach, the transformation method, the direct interpolation method, etc. In the present work, the penalty approach has been used to enforce essential boundary condition. Furthermore size of the penalty factor affects on accuracy of solutions. In the following determination of penalty factor are discussed.

Because discretization errors can be comparable in magnitude to the errors due to the poor satisfaction of the constraint, Zienkiewicz (1989) has suggested using the following formula for FEM analysis:

$$\alpha = const \quad \left(\frac{1}{h}\right)^n \quad (26)$$

Where h is the characteristic length, which can be the ratio of the element size to the dimension of the problem domain, and n is the order of the elements.

In extending this formula to meshless methods, we suggest that h be the ratio of the nodal spacing to the dimension of the problem domain, and n=1. The constant in Eq. (26) should relate to the material property of the solid or structure. It can be 10^{10} times Young's modulus.

This paper prefers the following simple method for determining the penalty factor:

$$\alpha = 1.0\times10^{4-13}\times \text{max.(diagonal elements in the stiffness matrix)} \quad (27)$$

In most of the examples reported using penalty methods, the foregoing equation is adopted.

It has also been suggested to use

$$\alpha = 1.0\times10^{5-8}\times \text{Young Modulus} \quad (28)$$

For some examples which work well.

Note that trials may be needed to choose a proper penalty factor.

5 RESULTS OF NUMERICAL EXAMPLES

In this section the meshless local Petrov–Galerkin method is applied to compute two-dimensional steady-state heat conduction problems. Results of three examples are compared with analytical solution.

We used 6 Gauss points for numerical evaluation of line integrals and a 4 * 4 quadrature scheme (i.e., 16 Gauss points) to evaluate domain integrals.

A. Example 1

We use these boundary conditions for Poisson' equation as (see Fig.3)

$$\begin{aligned} &\theta = 0 && at && x = 0 \\ &\theta = 0 && at && x = a \\ &\theta = \sin(x) && at && y = 0 \\ &\theta = 0 && at && y = b \end{aligned} \quad (29)$$

The analytical solutions for this problem are

$$\theta(x,y)=\frac{\sinh(\pi-y)\sin(x)}{\sinh(\pi)} \quad (30)$$

$$q_x(x,y)=\lambda\frac{\sinh(\pi-y)\cos(x)}{\sinh(\pi)} \quad (31)$$

$$q_y(x,y)=-\lambda\frac{\cosh(\pi-y)\sin(x)}{\sinh(\pi)} \quad (32)$$

The node distribution with 49 nodes are presented in Fig. 4 for the case of a=b= π .
The temperature distributions are presented in Fig. 5 and Fig. 6. The heat flux distributions are presented in Fig. 7 and Fig. 8.
As shown in these figures, the MLPG results agree with the values obtained by analytical solution. The convergence of the MLPG approach is demonstrated in these figures.

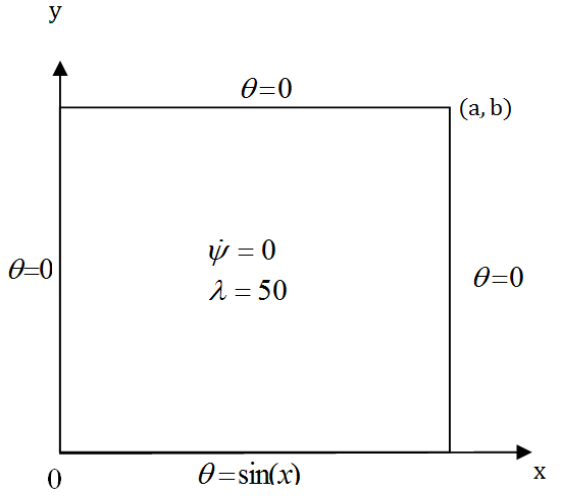

Fig. 3 Geometry and boundary conditions used for example 1

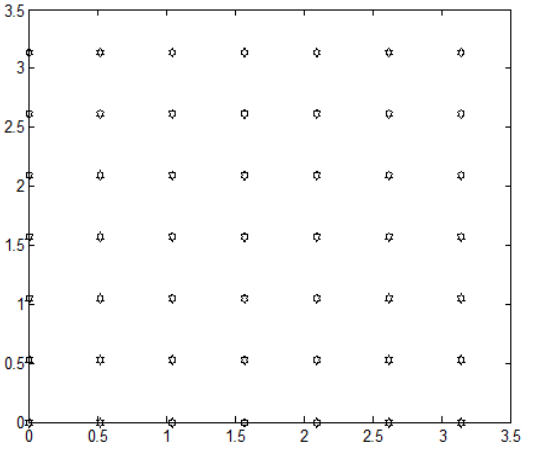

Fig. 4 Regular node distribution for example 1

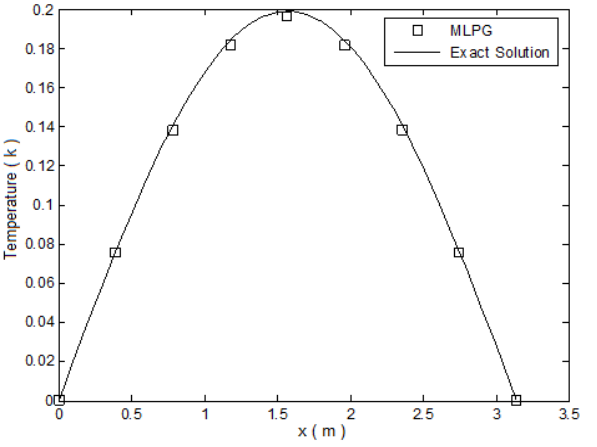

Fig. 5 Comparison of temperature distribution along y= $\frac{\pi}{2}$

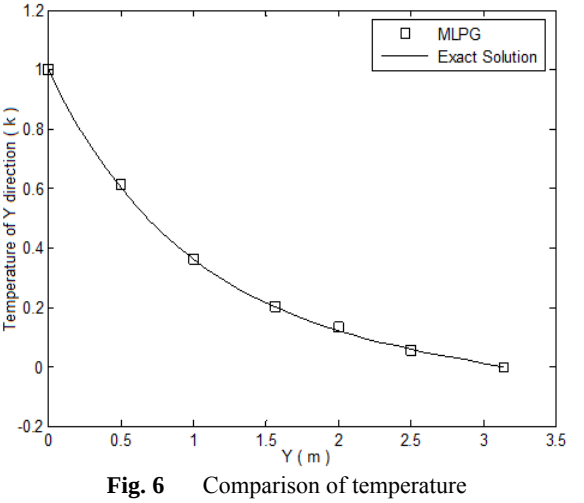

Fig. 6 Comparison of temperature distribution along x= $\frac{\pi}{2}$

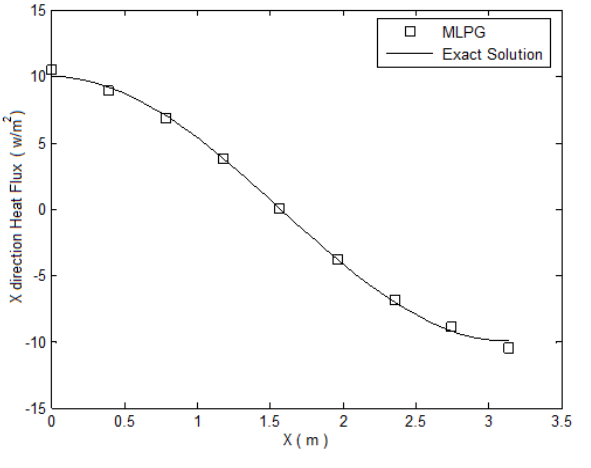

Fig. 7 Comparison of heat flux distribution along y= $\frac{\pi}{2}$

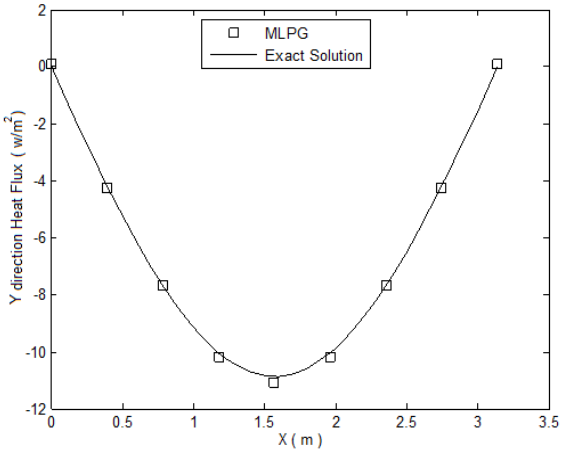

Fig. 8 Comparison of heat flux distribution along y=$\frac{\pi}{2}$

B. Example 2

In this case boundary conditions imposed are presented in Fig. 9 as

$$\begin{aligned} q_x &= 0 && at && x = 0 \\ q_x &= -\lambda \sin(y) && at && x = \pi \\ \theta &= 0 && at && y = 0 \\ \theta &= 0 && at && y = \pi \end{aligned} \tag{33}$$

The exact solutions for this problem are

$$\theta(x,y) = \frac{\cosh(x)\sin(y)}{\sinh(\pi)} \tag{34}$$

$$q_x(x,y) = \lambda \frac{\sinh(x)\sin(y)}{\sinh(\pi)} \tag{35}$$

$$q_y(x,y) = \lambda \frac{\cosh(x)\cos(y)}{\sinh(\pi)} \tag{36}$$

The node distribution with 100 nodes are presented in Fig. 10 for the case of a=b=π .
The temperature distribution is presented in Fig. 11 and the heat flux distributions are presented in Fig. 12.
As shown in these figures, the MLPG results agree with the values obtained by analytical solution.

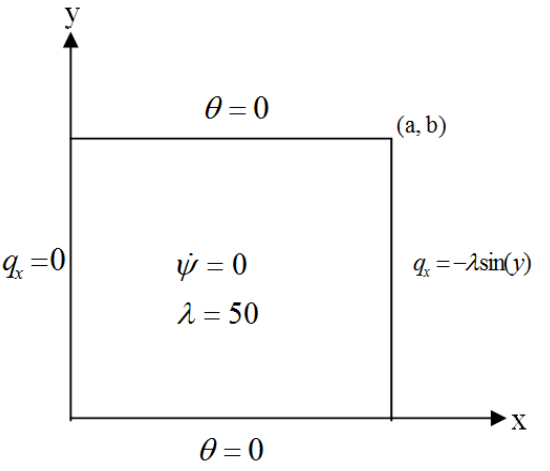

Fig. 9 Geometry and boundary conditions used for example 2

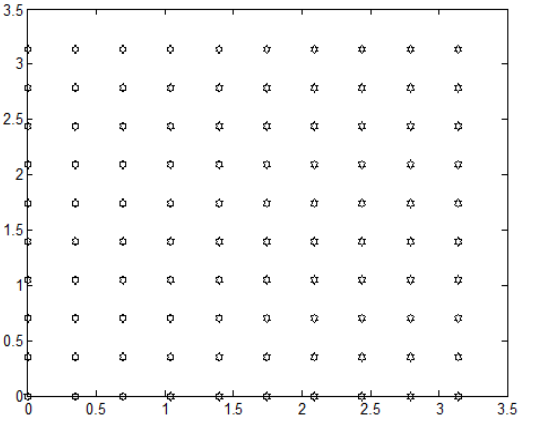

Fig. 10 Regular node distribution for example 2

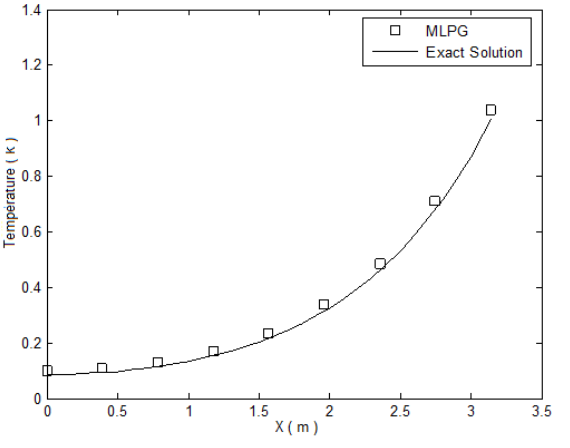

Fig. 11 Comparison of temperature distribution along y=$\frac{\pi}{2}$

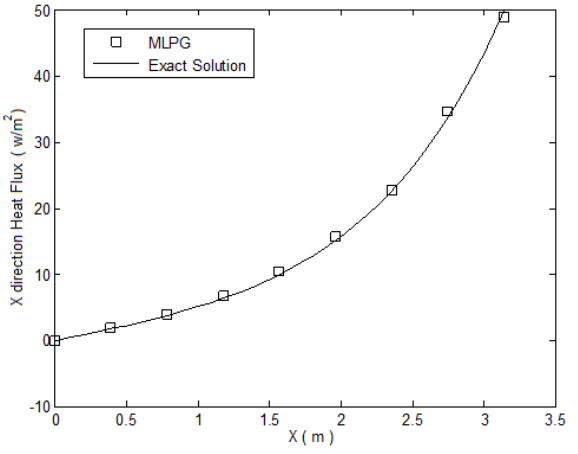

Fig. 12 Comparison of heat flux distribution along y=$\frac{\pi}{2}$

C. Example 3

In this example the MLPG approach is applied for heat conduction problem with boundary conditions imposed as (see Fig. 13)

$$\begin{aligned} q_x &= 0 && at && x = 0 \\ \theta &= x^2 && at && x = a \\ q_y &= 0 && at && y = 0 \\ \theta &= y^2 && at && y = b \end{aligned} \quad (37)$$

The analytical solutions for this problem are

$$\theta(x,y) = x^2 + y^2 - 1 \quad (38)$$

$$q_x(x,y) = 2\lambda x \quad (39)$$

$$q_y(x,y) = 2\lambda y \quad (40)$$

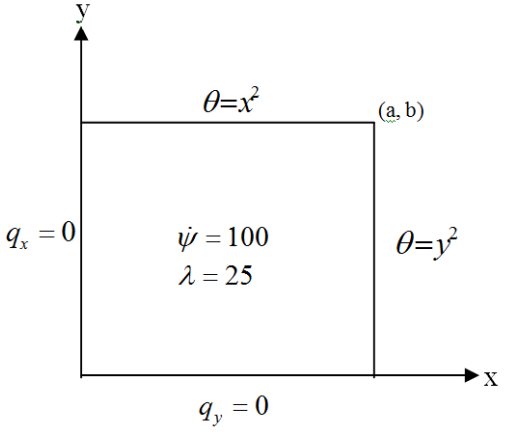

Fig. 13 Geometry and boundary conditions used for example 3

The node distribution with 25 nodes are presented in Fig. 14 for the case of a=b=1.
The temperature distribution is presented in Fig. 15 and the heat flux distribution is presented in Fig. 16.
As shown in this figure, the convergence of the MLPG approach is demonstrated.

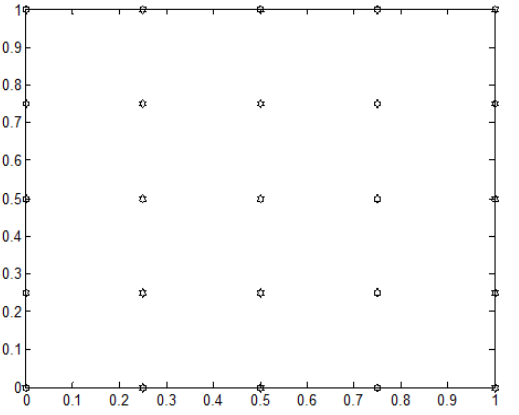

Fig. 14 Regular node distribution for example 3

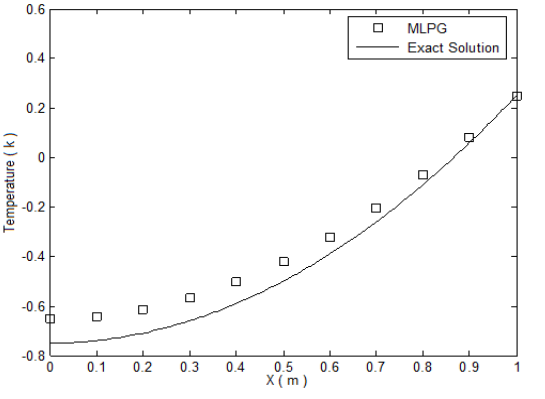

Fig. 15 Comparison of temperature distribution along y=1/2

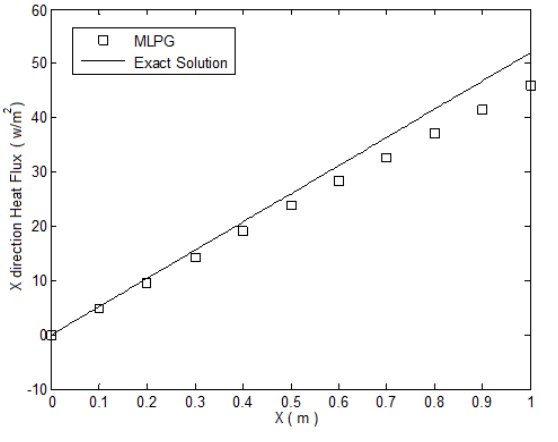

Fig. 16 Comparison of heat flux distribution along y=1/2

D. Example 4

In this example the MLPG approach is applied for heat conduction problem with boundary conditions imposed as (see Fig. 17)

$$\begin{aligned} q_x &= 0 \quad at \quad x = 0 \\ q_x &= 0 \quad at \quad x = a \\ \theta &= 0 \quad at \quad y = 0 \\ \theta_f &= 21 \,\&\, h = 8 \quad at \quad y = b \end{aligned} \tag{41}$$

The exact solutions for this problem are

$$\theta(x, y) = y^2 \tag{42}$$

$$q_x(x, y) = 0 \tag{43}$$

$$q_y(x, y) = 2\lambda y \tag{44}$$

The node distribution with 25 nodes are presented in Fig. 18 for the case of a=b=1.

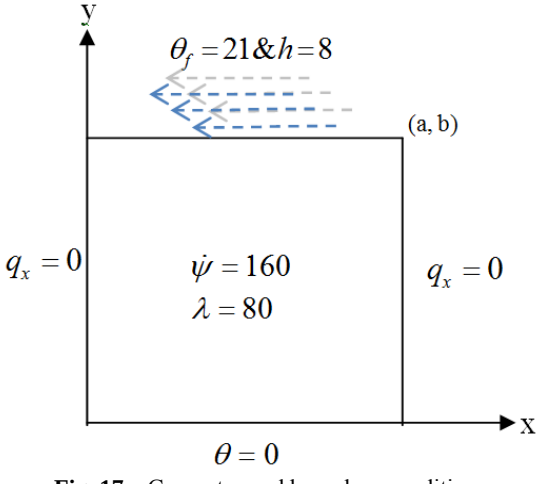

Fig. 17 Geometry and boundary conditions used for example 4

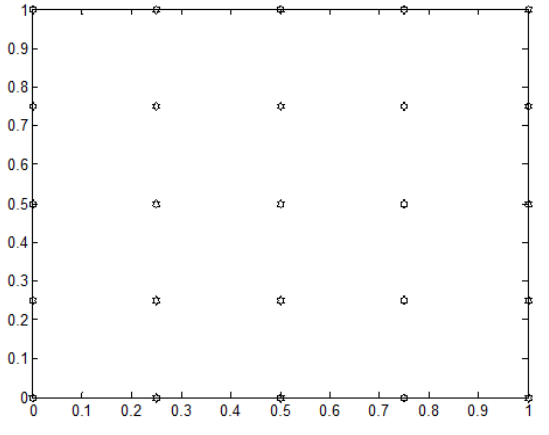

Fig. 18 Regular node distribution for example 4

The temperature distribution is presented in Fig. 19. The heat flux distribution is presented in Fig. 20. As shown in these figures, the results agree with the exact solution. The convergence of this approach is demonstrated in these figures.

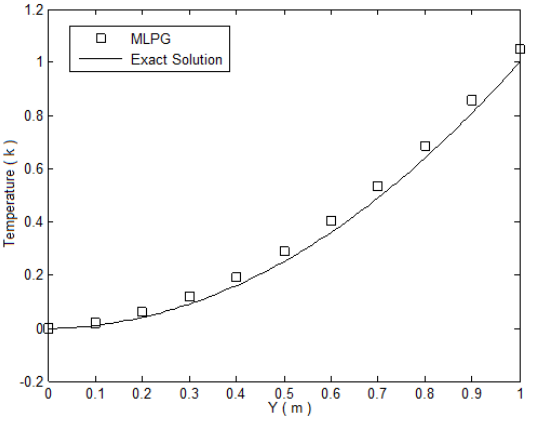

Fig. 19 Comparison of temperature distribution along x=1/2

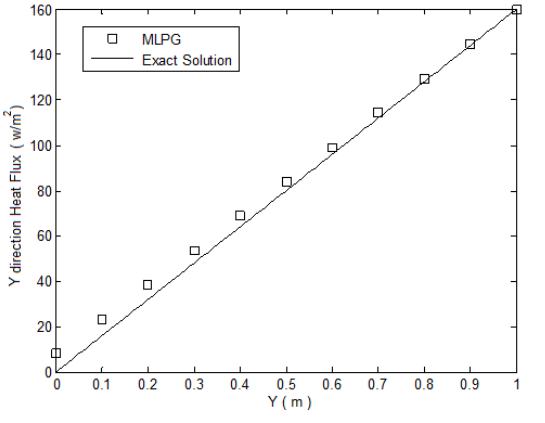

Fig. 20 Comparison of heat flux distribution along x=1/2

6 CONCLUSION

The meshless local Petrov–Galerkin (MLPG) method that uses a Heaviside test function is presented and used to analyze heat conduction problems. By using a Heaviside test function, the domain integral in the weak form is simplified. This substantially reduces the computation effort to construct the stiffness matrix and hence is computationally efficient compared to the conventional MLPG method. The penalty approach is used to impose the essential boundary conditions and the moving least squares approximation is used for interpolation schemes. The present results show that the MLPG algorithm with a Heaviside test function is a high convergence, good accurate and efficient method.

REFERENCES

[1] Atluri, S. N. and Zhu, T., "A New Meshless Local Petrov–Galerkin (MLPG) Approach in Computational Mechanics," Comput. Mech., Vol. 24, 1998, pp. 348–372.

[2] Lin H., Atluri and S. N., "Meshless Local Petrov-Galerkin (MLPG) Method for Convection-Diffusion Problems," CMES: Computer Modeling in Engineering & Sciences, Vol. 1, No. 2, 2000, pp. 45-60.

[3] Wu, Y. L., Liu, G. R. and Gu, Y. T., "Application of Meshless Local Petrov–Galerkin (MLPG) Approach to Simulation of Incompressible Flow," Numerical Heat Transfer, Part B, Vol. 48, 2005, pp. 459-475.

[4] Ching H. K. and Batra, R. C., "Determination of Crack Tip Fields in Linear Elastostatics by the Meshless Local Petrov-Galerkin (MLPG) Method," CMES: Computer Modeling in Engineering & Sciences, Vol. 2, No. 2, 2001, pp. 273-290.

[5] Long, S. Y. and Atluri, S. N., "A Meshless Local Petrov-Galerkin (MLPG) Method for Solving the Bending Problem of a Thin Plate," CMES: Computer Modeling in Engineering & Sciences, Vol. 3, No. 1, 2002, pp 53-63.

[6] Cleary, P. W. and Monaghan, J. J., "Conduction Modeling Using Smoothed Particle Hydrodynamics," J. Comput. Phys, Vol. 148, 1999, pp. 27–264.

[7] Qian, L. F. and Batra, R. C., "Three Dimensional Transient Heat Conduction in a Functionally Graded Thick Plate with a High Order Plate Theory and a Meshless Local Petrov Galerkin Method," Comput. Mech., Vol. 35, 2005, pp. 214–226.